Journal of the Physical Society of Japan
Vol. 77, No. 9, September, 2008, 093701

Magnetic Anisotropy of Paramagnetic and Ferromagnetically Ordered State of Single Crystal $BaVSe_3$

Mirta HERAK*, Marko MILJAK, Ana AKRAP[1], László FORRÓ[1], and Helmuth BERGER[1]

Institute of Physics, POB-304, HR-10000 Zagreb, Croatia
[1]*Institute de Physique de la Matière Complexe, EPFL, CH-1015 Lausanne, Switzerland*

(Received May 26, 2008; accepted July 9, 2008; published August 25, 2008)

Anisotropic magnetism of single crystal $BaVSe_3$ was studied for the first time by the combination of the susceptibility and torque methods. As reported previously for polycrystalline sample, $BaVSe_3$ undergoes ferromagnetic ordering below 43 K. Well above ferromagnetic ordering temperature, the torque measurements reveal a continuous symmetry change that influences the ordered state accordingly. We found ferromagnetic easy axis in the vanadium chain direction, i.e., along the crystallographic *c*-axis. The presence of two ferromagnetic domains of opposite magnetization direction signifies uniaxial symmetry of the ordered ferromagnetic state.

KEYWORDS: $BaVSe_3$, magnetic anisotropy, ferromagnetism, transition metal chalcogenide
DOI: 10.1143/JPSJ.77.093701

The compounds containing transition metal elements display a variety of interesting physical phenomena most of which are related to the existence of unpaired *d* electrons. Depending on the dimensionality of the crystal lattice and the spin state of the *d* electron of transition metal ion, a number of different ground states is observed in these compounds: nonmagnetic spin dimers and alternating spin chains, spin and charge density waves, colinear and noncolinear antiferromagnetic long range order, etc. $BaVSe_3$ contains vanadium d^1 electrons and thus belongs to the above mentioned class of compounds, just like widely studied $BaVS_3$.[1–9)]

$BaVSe_3$ is isostructural to $BaVS_3$.[10)] At high temperatures $BaVX_3$ (X = Se, S) forms a hexagonal perovskite type structure of $P6_3/mmc$ symmetry and at $T_s \approx 310$ K (240 K) $BaVSe_3$ ($BaVS_3$) exhibits a structural phase transition to orthorhombic symmetry, space group $Cmc2_1$, shown in Fig. 1. The parameters of the orthorombic unit cell in $BaVSe_3$ are $a = 6.992(2)$ Å, $b = 12.113(3)$ Å, and $c = 5.859(1)$ Å.[11)] Vanadium ions V^{4+} are surrounded by six Se ions forming a distorted octahedron. VSe_6 octahedra form zig-zag chains along *c*-axis by sharing the faces of the octahedra making $BaVSe_3$ a structurally one-dimensional (1D) system. Magnetic and transport properties of polycrystalline $BaVSe_3$ were reported previously.[12)] Unlike $BaVS_3$ which exhibits metal-to-insulator transition (MIT) $BaVSe_3$ is metallic from room temperature down to the lowest measured temperature of 2 K.[12,13)] The metallic behaviour in the entire temperature range, however, is observed in $BaVS_3$ under pressure. 1D lattice fluctuations as a precursor to the MIT persist in $BaVS_3$ up to 170 K[3)] and at low temperatures distortion of VS_6 octahedra takes place both in nonmagnetic ($T_X < T < T_{MIT}$) and magnetic phase ($T < T_X$).[9)] Magnetic susceptibility of $BaVSe_3$ displays paramagnetic Curie–Weiss (CW) behaviour at high temperatures and at $T_c \approx 43$ K the sample undergoes a transition to the ferromagnetically ordered state. Contrary to that, $BaVS_3$ orders antiferromagnetically below $T \approx 30$ K as evidenced from torque measurements[1)] and powder neutron diffraction experiment.[2)]

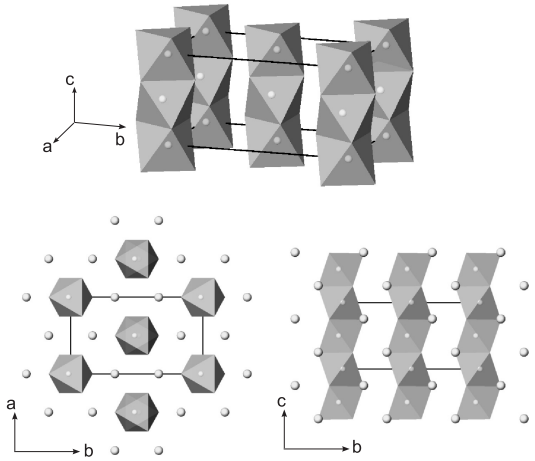

Fig. 1. Top: Crystal structure of $BaVSe_3$. Gray octahedra represent VSe_6 octahedra with light V atoms in the middle. Selenium atoms in the vertices of octahedra and barium atoms are not shown for the sake of clarity. Bottom, left: *ab* crystal plane. Large light spheres represent Ba atoms. Bottom, right: *bc* plane with VSe_6 zig-zag chains along *c*-axis.

Sulfur deficient $BaVS_{3-\delta}$ also orders ferromagnetically but two different vanadium sites (magnetic and nonmagnetic) are present in those samples. NMR experiment suggests there is a single magnetic V site in $BaVSe_3$ below T_c.[12)] In $BaVS_3$ under pressure MIT is suppressed and at $p \gtrsim 2.0$ GPa $BaVS_3$ becomes metallic in the whole temperature range.[14)] Se ions are larger than S ions which is why the interchain orbital overlap is increased in $BaVSe_3$ making the situation similar to the one in $BaVS_3$ under pressure. The magnetic phase of $BaVS_3$ is difficult to probe under pressure, which is why a study of magnetic properties of $BaVSe_3$ is useful.

In this Letter magnetic properties of single crystals of $BaVSe_3$ are described as probed by static magnetic susceptibility and torque measurements. Magnetic anisotropy of both paramagnetic (PM) and ferromagnetic (FM) state is described.

The $BaVSe_3$ single crystals were grown by using a standard solid-state reaction technique, as described elsewhere.[10)] The temperature dependence of magnetic suscepti-

*E-mail: mirta@ifs.hr

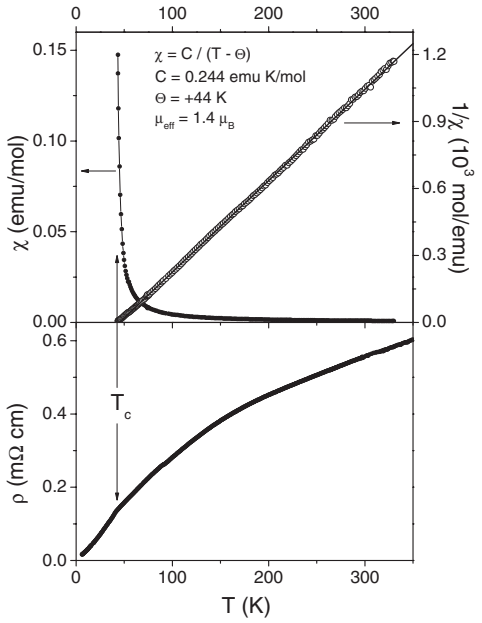

Fig. 2. Top: Magnetic susceptibility in PM phase and inverse susceptibility with fit to CW law. Bottom: Temperature dependence of resistivity measured along c crystallographic axes. The arrow marks the temperature of the ferromagnetic transition, T_c.

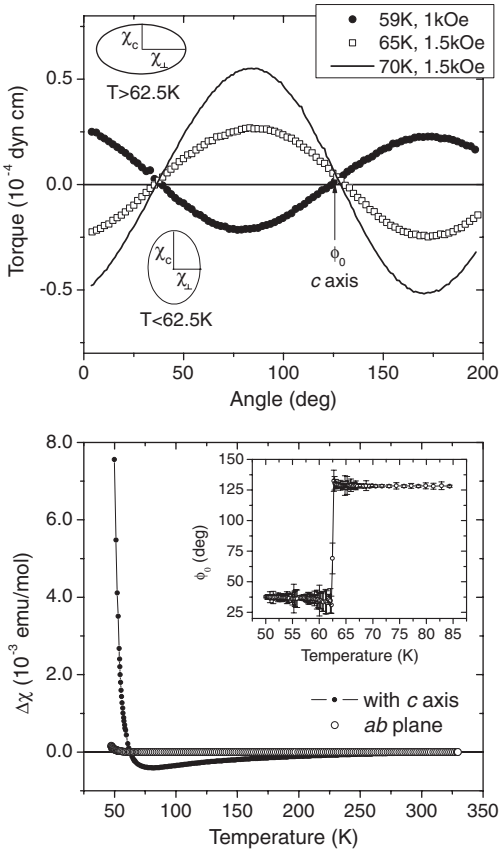

Fig. 3. Rotation of magnetic axes. Top: Torque curve at several different temperatures in PM state measured in the field plane containing axis c. Schematic presentation of susceptibility ellipsoid in the field plane is also shown for two cases realized at different temperatures. χ_c is susceptibility along c-axis, and $\chi_\perp$ is the one in the direction perpendicular to it in the field plane. Bottom: Temperature dependence of paramagnetic anisotropy in ab plane and plane containing c-axis. Inset: Temperature dependence of ϕ_0 — zero crossing of torque curve (see above).

bility in paramagnetic regime was measured by Faraday method in applied field of 9 kOe. The sample used to measure the susceptibility consisted of a bunch of randomly oriented single crystals of total mass $m = 0.004$ g. Temperature, field and angular dependence of magnetic torque were measured by home made torque apparatus. Two samples of different masses were used due to large signal in FM state. Mass of the sample used for measurements in PM state was 60 μg and for FM state (7 ± 2) μg. In FM state fields of up to 500 Oe were applied, and in PM state up to 8 kOe.

Raw susceptibility data in the paramagnetic state and corresponding CW plot are displayed in the top panel of Fig. 2. In the large temperature range susceptibility obeys CW law $\chi = C/(T - \Theta)$ with $C = 0.244$ emu K/mol and positive Weiss temperature $\Theta = +44$ K signifying the presence of ferromagnetic interactions. The magnetic moment obtained from CW plot amounts to $\approx 1.4 \mu_B$/f.u. which is close to the value obtained in ref. 12 for the polycrystalline sample. The single crystal orders ferromagnetically at $T_c \approx 43$ K, as reported previously.[12)] The temperature dependence of the resistivity of $BaVSe_3$ along c crystallographic axes, shown in the bottom panel of Fig. 2, is metallic in the whole range. The quasi-linear dependence above ~200 K is replaced by a faster decrease below this temperature. At T_c, a clear break in the slope can be seen. The detailed results will be published elsewhere.[13)]

Additional information of both PM and FM states is available from the symmetry sensitive torque measurements. In the PM state induced magnetization $\mathbf{M}$ depends linearly on the magnetic field $\mathbf{H}$: $M_i = \sum_j \chi_{ij} H_j$ where χ_{ij} is the susceptibility tensor, and $i(j) = x, y, z$. Magnetic torque $\mathbf{\Gamma}$ on the sample of volume V is given by the relation:

$$\mathbf{\Gamma} = V\,\mathbf{M} \times \mathbf{H} \qquad (1)$$

Evaluation of the component of torque Γ_k in the case of the paramagnetic response gives:

$$\Gamma_k = \frac{m}{2M_{\mathrm{mol}}} \Delta\chi_{i,j} H^2 \sin(2\phi - 2\phi_0), \qquad (2)$$

where m is the mass of the sample, M_{mol} is the molar mass, $\Delta\chi_{i,j} = \chi_i - \chi_j$ is the susceptibility anisotropy in the plane perpendicular to the measured torque Γ_k which is the plane of the rotation of the field H (i.e., the field plane), ϕ is the field goniometer angle. The phase shift ϕ_0 marks the direction of the crystal magnetic axis, manifested as the zero crossing of the torque sine curve i.e., marks the coincidence of the field direction and direction of the magnetic axis. Thus, the change of underlying magnetic symmetry reflects on experimental parameter ϕ_0. Note that precise directions of a- and b-axes with respect to the sample morphology were not available.

The top panel of Fig. 3 displays the angular torque dependence in PM state for the sample orientation that includes c-axis in the field plane measured at several temperatures and fields. The angle ϕ_0 corresponding to c-axis is marked in the figure. Measured field dependence of the torque satisfies equation (2) for $T \gtrsim 55$ K which means that the response of the system is paramagnetic in that

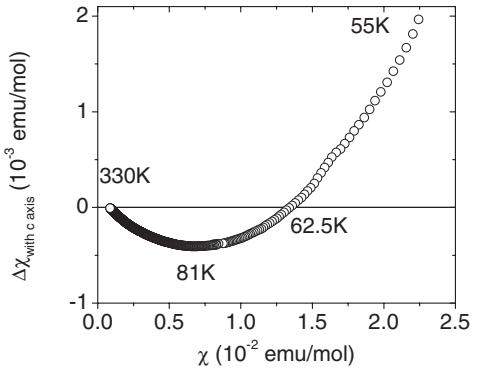

Fig. 4. Correlation of anisotropy and magnetic susceptibility in the PM state of $BaVSe_3$. At $T = 81$ K the curve changes the sign of the slope and at $T = 62.5$ K anisotropy $\Delta\chi$ changes sign.

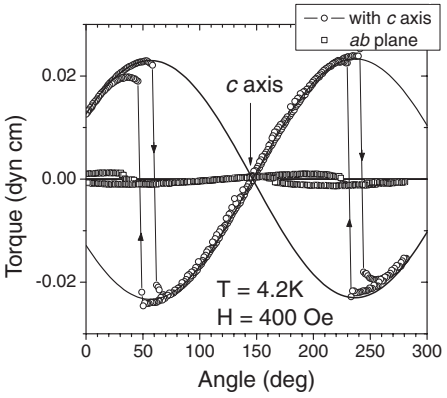

Fig. 5. Angle dependence of torque in FM state measured for two orientations of the sample.

temperature range (M is linear in H), while the torque field dependence at $T = 54$ K (not shown) still reflects reminiscence of the short-range order. The most important result, emphasizing symmetry change, is the phase difference of almost 90° between the torque sine curves obtained at $T \leq 60$ K and $T \geq 65$ K. Detailed temperature dependence of the phase difference is shown in the inset of the bottom panel of Fig. 3. The abrupt change of the angle ϕ_0 at 62.5 K does not correspond to a sharp transition since discontinuity in anisotropy is missing (see bottom panel of Fig. 3). At this temperature the torque amplitude becomes zero i.e., the system is fully isotropic. That is sketched in the top panel of Fig. 3 by showing the shape of the susceptibility ellipsoid (i.e., ellipse) in the field plane for temperatures above and below $T \approx 62.5$ K. Above 62.5 K the susceptibility χ_c is smaller than the susceptibility perpendicular to it in the field plane, $\chi_\perp$, $\chi_c < \chi_\perp$. At temperatures below 62.5 K $\chi_c > \chi_\perp$. At $T \approx 62.5$ K ellipse becomes a circle, i.e., $\chi_c = \chi_\perp$. Using eq. (2) evaluated anisotropy at $T = 300$ K for *ab* plane amounts to $\Delta\chi_{ab}(300\,\text{K}) = 6.5 \times 10^{-7}$ emu/mol and in the plane containing c-axis $\Delta\chi_{\text{with}\,c}(300\,\text{K}) = 2 \times 10^{-5}$ emu/mol. Regarding the known torque-method setup geometry (field direction and the orientation of the sample in the field) and rather small anisotropy in the *ab* plane, we found that $\chi_c > \chi_\perp$ below 62.5 K while the system is still in the PM phase with no FM fluctuations present yet. Considering susceptibility, which follows CW law down to at least 50 K, it is surprising that the anisotropy displays a local extremum at about $T \approx 80$ K. In the case of paramagnetic susceptibility, the susceptibility anisotropy results from the temperature independent electron g-factor anisotropy, $\Delta\chi_{i,j} = \langle\chi\rangle \times (g_i^2 - g_j^2)/\langle g\rangle^2$. Figure 4 displays $\Delta\chi$ vs $\langle\chi\rangle$ in the PM state showing no linear correlation between the two. This suggests the changes in symmetry occur in a rather wide temperature range in PM state. On the other hand, all effects of the crystal symmetry change at $T_s = 310$ K reflect only in rather small change of slope in $\Delta\chi(T)$ data (not shown).

The details of FM ordered state below $T_c = 43$ K were probed by torque measurements in fields up to 500 Oe at $T = 4.2$ K for both sample orientations as in PM state. Angular dependence is presented in Fig. 5. Note the 20 times smaller amplitude observed in the *ab* plane compared to plane with c-axis. The observed torque sine curves can be described by two regular sine curves $\sim \sin(\phi - \phi_0)$ differing

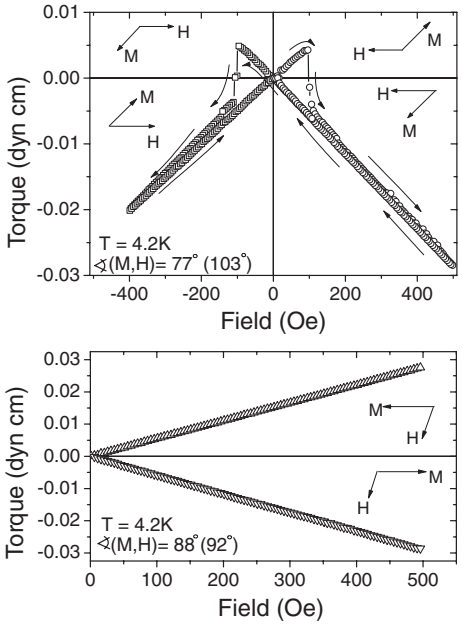

Fig. 6. Field dependence of torque in the FM state measured at two different angles in plane containing axis c.

in phase by 180°, as shown in Fig. 5. The half period of the experimental sine curves of 180°, together with torque definition (1), proves that the torque results from field independent, i.e., spontaneous magnetization. Furthermore, the torque curve shows that the ferromagnetic easy axis is parallel to the c crystallographic axis, within experimental resolution of 1°. The torque field dependence in case of spontaneous magnetization should follow linear field dependence, until the field reaches the switching value H_c. The field dependence of torque at two different angles is shown in Fig. 6. The top panel represents data obtained with field goniometer angle of 70° and the bottom panel with 55° (for values of torque at those angles consult Fig. 5). The bottom panel displays two linear field dependences for the same field angle away from the switching angle and the same field polarity. The only difference was that lower (negative) data was collected after the sample had some history including the switching effect that left the spontaneous magnetization oriented oppositely in respect to the

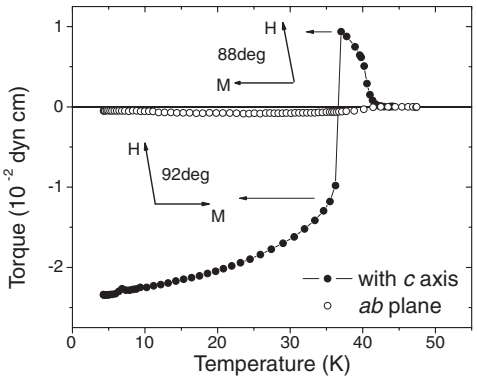

Fig. 7. Temperature dependence of torque in the FM state for two different sample orientations.

first (positive) data. The angles between **M** and **H** are shown schematically in the figure. From the series of such measurements the critical field applied in the direction opposite to the magnetization needed for reorientation of FM domains was estimated to be $H_c \approx 20$ Oe. Demagnetization effects in ferromagnets are usually significant. However, in the needle shape geometry of $BaVSe_3$ with the longest dimension along c-axis which is also the direction of FM magnetization, demagnetization effects are expected to be largely reduced.

The temperature dependence of torque measured in applied field of 400 Oe for two sample orientations is shown in Fig. 7. The torque in the plane containing c-axis was measured from 4.2–50 K after measuring the negative curve in the bottom panel of Fig. 6 with the same field polarity and at the same angle. For this **M** and **H** geometry magnetization should switch to opposite direction, but at low temperatures the field does not reach critical value. At higher temperatures the switching is thermally activated and torque changes sign consequently. Torque in ab plane is 20 times smaller and probably is the contribution of the domain walls. Another possibility is that the spontaneous magnetization has a small ab plane component. The torque in Fig. 7 has a characteristic order parameter temperature dependence. Assuming single-domain FM state for the fields $H > H_c$, the effective magnetic moment at 4.2 K amounts to $\mu_{\text{eff}} = (0.6 \pm 0.2)\mu_B$ from torque measurements (large value of uncertainty comes from the uncertainty of the small mass). Similar reduced value of $\mu_{\text{eff}} = 0.34$ is obtained in ref. 12 from the Arrot plot while from NMR data the same authors obtained $\mu_{\text{eff}} = 0.61\mu_B$ with assumption on equality of hyperfine interaction with $BaVS_3$.

In conclusion, single crystalline $BaVSe_3$ was studied by static magnetic susceptibility and torque measurements. Magnetic susceptibility obeys Curie–Weiss law emphasizing moderate FM interaction. From torque measurements we evaluate reduced effective magnetic moment of $\mu_{\text{eff}} = (0.6 \pm 0.2)\mu_B$ and give first evidence of the uniaxial symmetry of the ferromagnetic ordered state. We found evidence of symmetry changes in the wide temperature range of paramagnetic phase.

Acknowledgments

The work in Zagreb was supported by the resources of the SNSF-SCOPES (Scientific Co-operation between Eastern Europe and Switzerland) project and by the Croatian Ministry of Science, Education and Sports under Grant No. 035-0352843-2846. The work in Lausanne was sponsored by the Swiss National Science Foundation and its NCCR MaNEP.

1) G. Mihály, I. Kézsmárki, F. Zámbrosky, M. Miljak, K. Penc, P. Fazekas, H. Berger, and L. Forró: Phys. Rev. B **61** (2000) R7831.
2) H. Nakamura, T. Yamasaki, S. Giri, H. Imai, M. Shiga, K. Kojima, M. Nishi, K. Kakurai, and N. Metoki: J. Phys. Soc. Jpn. **69** (2000) 2763.
3) S. Fagot, P. Foury-Leylekian, S. Ravy, J.-P. Pouget, and H. Berger: Phys. Rev. Lett. **90** (2003) 196401.
4) T. Inami, K. Ohwada, H. Kimura, M. Watanabe, Y. Noda, H. Nakamura, T. Yamasaki, M. Shiga, N. Ikeda, and Y. Murakami: Phys. Rev. B **66** (2002) 073108.
5) F. Lechermann, S. Biermann, and A. Georges: Phys. Rev. Lett. **94** (2005) 166402.
6) S. Fagot, P. Foury-Leylekian, S. Ravy, J.-P. Pouget, É. Lorenzo, Y. Joly, M. Greenblatt, M. V. Lobanov, and G. Popov: Phys. Rev. B **73** (2006) 033102.
7) S. Mitrovic, P. Fazekas, C. Søndergaard, D. Ariosa, N. Barišić, H. Berger, D. Cloëtta, L. Forró, H. Höchst, I. Kupčić, D. Pavuna, and G. Margaritondo: Phys. Rev. B **75** (2007) 153103.
8) F. Lechermann, S. Biermann, and A. Georges: Phys. Rev. B **76** (2007) 085101.
9) S. Fagot, P. Foury-Leylekian, S. Ravy, J.-P. Pouget, M. Anne, G. Popov, M. V. Lobanov, and M. Greenblatt: Solid State Sci. **7** (2005) 718.
10) J. Kelber, A. H. Reis, Jr., A. T. Aldred, M. H. Mueller, O. Massenet, G. DePasquali, and G. Stucky: J. Solid State Chem. **30** (1979) 357.
11) N. J. Poulsen: Mater. Res. Bull. **33** (1998) 313.
12) T. Yamasaki, S. Giri, H. Nakamura, and M. Shiga: J. Phys. Soc. Jpn. **70** (2001) 1768.
13) A. Akrap, V. Stevanović, M. Herak, M. Miljak, N. Barišić, H. Berger, and L. Forró: unpublished.
14) N. Barišić, A. Akrap, H. Berger, and L. Forró: arXiv:0712.3395.